Original article

Identification of novel molecular scaffolds for the design of MMP-13 inhibitors: A first round of lead optimization

Valeria La Pietra [a,1], Luciana Marinelli [a,*,1], Sandro Cosconati [b], Francesco Saverio Di Leva [c], Elisa Nuti [d], Salvatore Santamaria [d,e], Isabella Pugliesi [d], Matteo Morelli [d], Francesca Casalini [d], Armando Rossello [d], Concettina La Motta [d], Sabrina Taliani [d], Robert Visse [e], Hideaki Nagase [e], Federico da Settimo [d], Ettore Novellino [a,1]

[a] Dipartimento di Chimica Farmaceutica e Tossicologica, Università di Napoli "Federico II" Via D. Montesano 49, 80131 Napoli, Italy
[b] Dipartimento di Scienze Ambientali, Seconda Università di Napoli, Via Vivaldi 43, 81100 Caserta, Italy
[c] Department of Drug Discovery and Development, Istituto Italiano di Tecnologia (IIT), Via Morego 30, 16163 Genova, Italy
[d] Dipartimento di Scienze Farmaceutiche, Università di Pisa, via Bonanno 6, 56126 Pisa, Italy
[e] Department of Matrix Biology, The Kennedy Institute of Rheumatology Division, Imperial College, London, W6 8LH, United Kingdom

ARTICLE INFO

ABSTRACT

Osteoarthritis (OA) is the leading cause of joint pain and disability in middle-aged and elderly patients, and is characterized by progressive loss of articular cartilage. Among the various matrix metalloproteinases (MMPs), MMP-13 is specifically expressed in the cartilage of human OA patients and is not present in normal adult cartilage. Thus, MMP-13-selective inhibitors are promising candidates in osteoarthritis therapy. Recently, we designed an N-isopropoxy-arylsulfonamide-based hydroxamate inhibitor, which showed low nanomolar activity and high selectivity for MMP-13. In parallel to further studies aiming to assess the in vivo activity of our compound, we screened the Life Chemicals database through computational docking to seek for novel scaffolds as zinc-chelating non-hydroxamate inhibitors. Experimental evaluation of 20 selected candidate compounds verified five novel leads with IC_{50} in the low μM range. These newly discovered inhibitors are structurally unrelated to the ones known so far and provide useful scaffolds to develop compounds with more desirable properties. Finally, a first round of structure-based optimization on lead **1** was accomplished and led to an increase in potency of more than 5 fold.

1. Introduction

Osteoarthritis (OA) is the leading cause of joint pain and disability in middle-aged and elderly patients. It is characterized by progressive loss of articular cartilage that eventually leads to denudation of the joint surface. The cartilage loss observed in OA is the result of a complex process involving degradation of various components of the cartilage matrix. Particularly, degradation of cartilage-specific type II collagen by mammalian collagenases (MMPs) is a key step in the loss of structural and functional integrity of cartilage [1]. Among all known MMPs, MMP-13 is considered the principal target in OA. Indeed, today there are overwhelming data on the role of MMP-13 in the pathogenesis of OA [2], and inhibition of its activity has proven to be efficacious in a variety of models of experimentally induced as well as spontaneously occurring OA [3]. Unfortunately, none of the known MMP inhibitors (MMPIs) have been successfully utilized as therapeutic agents so far. This was due to the lack of selectivity for a specific isozyme, leading to heavy dose- and duration-dependent musculoskeletal side effects [4]. Therefore, current drug development strategies for treatment of OA are focused on selective inhibition of MMP-13, although recent evidences suggest that other MMPs, such as MMP-1, may also contribute to the collagen degradation process [5]. However, the design of a selective MMPI is not a trivial task, as MMPs share an high similarity in the overall three-dimensional fold and many conserved amino acids exist in the inhibitor binding site, besides the conserved catalytic zinc ion. The major structural difference observed between the MMP enzymes resides in the relative size and shape of the S1′ subsite, which is located in proximity of the catalytic metal. From a structural point of view,

* Corresponding author. Tel./fax: +39 081 678644.
  E-mail address: lmarinel@unina.it (L. Marinelli).
[1] Fax: +39 081 678619.

almost all MMPIs known so far are based on a zinc-binding group (ZBG) and a hydrophobic portion protruding into the hydrophobic S1′ subsite. These compounds behave as competitive inhibitors since the ZBG can mimic one of the transition states occurring during the substrate hydrolysis. Currently, two successful strategies to confer selectivity of action to an MMP13 inhibitor are known: the first resides in the proper modification of the P1′ substituent on MMPI to take advantage of the differences between the diverse MMPs; the second is the finding of an allosteric inhibitor [6], which binds tightly to the S1′* site, a unique side pocket adjacent to S1′ that hasn't been observed for other MMPs, without chelating the metal that is thought to contribute to the promiscuous inhibition of multiple MMPs. Recently, as a result of the first strategy, we designed a N-isopropoxy-arylsulfonamide-based hydroxamate inhibitor, which showed low nanomolar activity for MMP-13 and high selectivity over some other tested MMPs [7]. In parallel to further studies aiming to assess the activity of this promising compound using in vivo models of OA, we decided to seek for novel scaffolds as zinc-chelating non-hydroxamate inhibitors. In fact, a debate is still open on the advisability of using hydroxamates as ZBG due to toxicity and metabolic stability issues [8,9].

In this respect, we have taken advantage of the availability of several MMP-13 crystal structures and have used computational docking to screen the Life Chemicals database. Experimental tests of a limited selection of candidate compounds (20) verified five novel leads, structurally unrelated to the known MMPIs. A first round of structure-based optimization on lead **1** was accomplished and led to an increase in potency of more than 5 fold.

2. Experimental section

2.1. Database preparation

For the in silico screening, the Life Chemicals database [10] was used. This library is a collection of small compounds carefully selected to provide the broadest pharmacophore coverage for a total of six thousands non-redundant molecules. The database was uploaded on ZINC server [11] as 1D smiles strings and processed with the ZINC protocol. This protocol filters-out molecules with molecular weight greater than 700, calculated LogP greater than 6 and less than −4, number of hydrogen-bond donors, hydrogen-bond acceptors, and rotatable bonds greater than 6, 11, and 15 respectively. It also removes all molecules containing "exotic" atoms (i.e. different from H, C, N, O, F, S, P, Cl, Br, or I). Moreover it allows the creation of all stereoisomers, tautomers and correctly protonated forms of the molecules between pH 5 and 9.5. The protocol outcome from the server was a file containing 7769 compounds.

2.2. Selection of the MMP-13 X-ray structure for VS experiment and protein preparation

Several X-ray structures of MMP-13 have been released in the Protein Data Bank (PDB) so far. A superposition of all X-ray structures on the alpha carbon atoms, using 830C as reference structure, shows that the protein folding and the catalytic loops shape are highly superimposable and that in the catalytic site, the large majority of the residues are all preserved in the side chain conformations. Thus, only the enzyme structure 830C, which has the higher resolution (1.60 Å), was selected for our VS experiment. From this structure, all water molecules, ions and the inhibitor were removed from the binding site. All hydrogen atoms were added to the protein structure using ADT [12], and to the catalytic Zn ion present in the active site a +2 charge was assigned.

2.3. Virtual screening calculations

Docking calculations were performed with version 4.0 of the AutoDock software package as implemented through the graphic user interface AutoDockTools (ADT 1.4.6). All compounds of the Life Chemical diversity set together with the 830C structure of MMP-13 were converted to AutoDock format files (.pdbqt) using ADT. The docking area was defined by a box, centered on the catalytic zinc. Grids (dimension of 60 Å × 65 Å × 60 Å) were then generated for 13 ligand atom types (sufficient to describe all atoms in the selected database) with the help of AutoGrid4 using a grid spacing of 0.375 Å. For each ligand of the Life Chemical diversity set, 100 separate docking calculations were performed. Each docking calculation consisted of 1×10^7 energy evaluations using the Lamarckian genetic algorithm local search (GALS) method. A low-frequency local search in accordance with the method of Solis and Wets was applied to docking trials to ensure that the final solution represents a local minimum. Each docking run was performed with a population size of 150, and 300 rounds of Solis and Wets local search were applied, with a probability of 0.06. A mutation rate of 0.02 and a crossover rate of 0.8 were used to generate new docking trials for subsequent generations. The docking results from each of the 100 calculations were clustered on the basis of root-mean square deviation (rmsd 2 Å) between the Cartesian coordinates of the ligand atoms and were ranked on the basis of the free energy of binding. The top-ranked compounds were visually inspected for good chemical geometry. Finally, as a last criterion of selection, we introduced the visual inspection of the putative best ranking ligand/receptor complexes. In this regard, we decided to discard all the molecules for which AD4 did not predict coordination of the catalytic zinc in order to obtain compounds of a certain potency. Another selection criterion resided in the occupancy of the S1′ pocket, in the attempt to obtain a selectivity of action towards the MMP-13. Pictures of the modelled ligand/enzyme complexes together with graphic manipulations were rendered with UCSF chimera package from the Resource for Biocomputing, Visualization, and Informatics at the University of California, San Francisco [13].

2.4. Chemistry

The purity of the five hits that were essential to the conclusions drawn in the text were determined by HPLC on a Merck Hitachi D-7000 liquid chromatograph equipped with a Discovery C18 column (250 mm × 4.6 mm, 5 μm particle size) and a UV/vis detector setting at λ = 250 nm. All compounds were eluted with the solvent systems listed in Supporting Information Table 1.

As regards the newly synthesized compounds **1a**–**h** and their intermediates, melting points were determined using a Reichert Köfler hot-stage apparatus and are uncorrected. Routine nuclear magnetic resonance spectra were recorded in DMSO-d_6 solution on a Varian Gemini 200 spectrometer operating at 200 MHz. Analytical TLC was carried out on Merck 0.2 mm precoated silica gel aluminium sheets (60 F-254). Elemental analyses were performed by our Analytical Laboratory and agreed with theoretical values to within ±0.4%.

2-hydroxy-3-methoxybenzaldehyde, 2-hydroxy-5-methoxyben zaldehyde, 2,3-dihydroxybenzaldehyde, 5-chloro-2-hydroxyben zaldehyde, 5-chloro-2-hydroxy-3-methoxybenzaldehyde, 5-allyl-2-hydroxy-3-methoxybenzaldehyde, 3-(2-bromoacetyl)-2H-chro men-2-one (**6**), ethyl acetoacetate, aniline, 3-aminobenzoic acid, ethyl 3-aminobenzoate, reagent and solvents were from Sigma-Aldrich.

3-Acetyl-8-methoxy-2H-chromen-2-one (**21**) [14], 3-acetyl-6-methoxy-2H-chromen-2-one (**22**) [15], were obtained according to reported procedures.

3. General procedure for the synthesis of 6,8-substituted 3-acetyl-2*H*-chromen-2-one derivatives 23−26

A mixture of equimolar quantities (0.006 mol) of the appropriate salicylaldehyde (2,3-dihydroxybenzaldehyde, 5-chloro-2-hydroxybenzaldehyde, 5-chloro-2-hydroxy-3-methoxybenzaldehyde, 5-allyl-2-hydroxy-3-methoxybenzaldehyde) and ethyl acetoacetate in 15 mL of absolute ethanol was stirring in the presence of a few drops of piperidine for 5 h at room temperature (TLC analysis). After cooling, the precipitate which formed was collected to give the 3-acetyl-2*H*-chromen-2-one derivatives 23−26 which were purified by crystallization from ethanol.

3.1. 3-Acetyl-8-hydroxy-2H-chromen-2-one (23)

Yield: 63%; mp: 248−250 °C (ref. [16], mp: 253 °C). Anal. Calcd. for $C_{11}H_8O_4$: C, 64.71; H, 3.95; found: C, 64.99; H, 3.89.

3.2. 3-Acetyl-6-chloro-2H-chromen-2-one (24)

Yield: 69%; mp: 198−200 °C (ref. [17], mp: 204 °C). Anal. Calcd. for $C_{11}H_7ClO_3$: C, 59.35; H, 3.17; found: C, 59.59; H, 3.09.

3.3. 3-Acetyl-6-chloro-8-methoxy-2H-chromen-2-one (25)

Yield: 87%; mp: 189−191 °C; ^{1}H NMR (200 MHz, DMSO-d$_6$), δ: 2.58 (s, 3H); 3.96 (s, 3H); 7.46 (s, 1H); 7.63 (s, 1H); 8.59 (s, 1H). Anal. Calcd. for $C_{12}H_9ClO_4$: C, 57.05; H, 3.59; found: C, 57.29; H, 3.43.

3.4. 3-Acetyl-6-allyl-8-methoxy-2H-chromen-2-one (26)

Yield: 81%; mp: 147−149 °C; ^{1}H NMR (200 MHz, DMSO-d$_6$), δ: 2.57 (s, 3H); 3.37−3.45 (m, 2H); 3.96 (s, 3H); 5.08−5.17 (m, 2H); 5.95−6.023 (m, 1H); 7.27−7.29 (m, 2H); 8.58 (s, 1H). Anal. Calcd. for $C_{15}H_{14}O_4$: C, 69.76; H, 5.46; found: C, 69.99; H, 5.29.

4. General procedure for the synthesis of 6,8-substituted 3-(2-bromoacetyl)-2*H*-chromen-2-one derivatives 7−12

A hot solution of the appropriate 3-acetyl-2*H*-chromen-2-ones 21−26 (0.0022 mol) in chloroform was added to a suspension of copper (II) bromide (0.900 g, 0.0044 mol) in 10 mL of ethyl acetate. The resulting reaction mixture was refluxed with vigorous stirring to ensure complete exposure of the copper (II) bromide to the reaction medium until the reaction was complete, as judged by colour change of the solution from green to amber, disappearance of all black solid, and cessation of hydrogen bromide evolution. The suspension obtained was filtered to remove the copper (I) bromide. After cooling, the solid which separated was collected to give the 3-(2-bromoacetyl)-2*H*-chromen-2-ones 7−12, which were purified by crystallization from ethanol.

4.1. 3-(2-Bromoacetyl)-8-methoxy-2H-chromen-2-one (7)

Yield: 68%; mp: 199−201 °C (ref. [18], mp: 206 °C); ^{1}H NMR (200 MHz, DMSO-d$_6$), δ: 3.95 (s, 3H); 4.91 (s, 2H); 7.38−7.56 (m, 3H); 8.82 (s, 1H). Anal. Calcd. for $C_{12}H_9BrO_4$: C, 48.51; H, 3.05; found: C, 48.73; H, 2.98.

4.2. 3-(2-Bromoacetyl)-6-methoxy-2H-chromen-2-one (8)

Yield: 70%; mp: 135−137 °C; ^{1}H NMR (200 MHz, DMSO-d$_6$), δ: 3.83 (s, 2H); 4.91 (s, 2H); 7.40−7.58 (m, 3H); 8.79 (s, 1H) [19]. Anal. Calcd. for $C_{12}H_9BrO_4$: C, 48.51; H, 3.05; found: C, 48.68; H, 3.00.

4.3. 3-(2-Bromoacetyl)-8-hydroxy-2H-chromen-2-one (9)

Yield: 62%; mp: 223−225 °C; ^{1}H NMR (200 MHz, DMSO-d$_6$), δ: 4.89 (s, 2H); 7.23−7.29 (m, 2H); 7.37−7.44 (m. 1H); 8.76 (s, 1H); 10.47 (bs, 1H, OH, exch. with D$_2$O). Anal. Calcd. for $C_{11}H_7BrO_4$: C, 46.67; H, 2.49; found: C, 46.79; H, 2.42.

4.4. 3-(2-Bromoacetyl)-6-chloro-2H-chromen-2-one (10)

Yield: 60%; mp: 217−219 °C (ref. [20], mp: 221−222 °C). Anal. Calcd. for $C_{11}H_6BrClO_3$: C, 43.83; H, 3.01; found: C, 43.98; H, 2.92.

4.5. 3-(2-Bromoacetyl)-6-chloro-8-methoxy-2H-chromen-2-one (11)

Yield: 59%; mp: 218−220 °C; ^{1}H NMR (200 MHz, DMSO-d$_6$), δ: 3.97 (s, 3H); 4.90 (s, 2H); 7.54 (s, 1H); 7.67 (s, 1H); 8.76 (s, 1H). Anal. Calcd. for $C_{12}H_8BrClO_4$: C, 43.47; H, 2.43; found: C, 43.67; H, 2.35.

4.6. 6-Allyl-3-(2-bromoacetyl)-8-methoxy-2H-chromen-2-one (12)

Yield: 66%; mp: 156−158 °C; ^{1}H NMR (200 MHz, DMSO-d$_6$), δ: 3.38−3.55 (m, 2H); 3.92 (s, 3H); 4.88 (s, 2H); 5.08−5.17 (m, 2H); 5.95−6.02 (m, 1H); 7.32−7.38 (m, 2H); 8.74 (s, 1H). Anal. Calcd. for $C_{15}H_{13}BrO_4$: C, 53.43; H, 3.89; found: C, 53.27; H, 3.93.

5. General procedure for the synthesis of 3′,6,8-substituted 3-(2-phenylaminoacetyl)-2*H*-chromen-2-one derivatives 13−20

A solution of the opportune amine (aniline, 3-aminobenzoic acid, ethyl 3-aminobenzoate) (0.0021 mol), NaHCO$_3$ (0.176 g, 0.0021 mol) and the appropriately substituted α-bromocetyl-2*H*-chromen-2-ones 6−12 (0.0021 mol) in 10 mL of ethanol was refluxed for 5 h (TLC analysis). After cooling, the precipitate which formed was collected and derivatives 13−20 resulted sufficiently pure to be used in the next reaction without further purification.

5.1. 3-[2-(Phenylamino)acetyl]-2H-chromen-2-one (13)

Yield: 70%; mp: 177−179 °C (ref. [21], mp = 180−185 °C). ^{1}H NMR (200 MHz, DMSO-d$_6$), δ: 4.59 (d, 2H, J = 5.8 Hz); 5.94 (t, 1H, J = 5.6 Hz, exch. with D$_2$O); 6.52−6.63 (m, 3H); 7.04−7.12 (m, 2H); 7.40−7.53 (m, 2H); 7.68−7.82 (m, 1H); 7.97−8.01 (m, 1H); 8.75 (s, 1H). Anal. Calcd. for $C_{17}H_{13}NO_3$: C, 73.11; H, 4.69; N, 5.02; found: C, 73.27; H, 4.73; N, 4.97.

5.2. 3-[2-(3-Ethoxycarbonyl)phenylaminoacetyl]-2H-chromen-2-one (14)

Yield: 76%; mp: 175−177 °C; ^{1}H NMR (200 MHz, DMSO-d$_6$), δ: 1.29 (t, 3H, J = 7.0 Hz); 4.27 (q, 2H, J = 7.1 Hz); 4.65 (d, 2H, J = 4.2 Hz); 6.20 (t, 1H, J = 4.0 Hz, exch. with D$_2$O); 6.85−6.88 (m, 1H); 7.18−7.22 (m, 1H); 7.41−7.54 (m, 2H); 7.74−7.82 (m, 1H); 7.98−8.02 (m, 1H); 8.77 (s, 1H). Anal. Calcd. for $C_{20}H_{17}NO_5$: C, 68.37; H, 4.88; N, 3.99; found: C, 68.27; H, 4.73; N, 3.85.

5.3. 3-[2-(3-Hydroxycarbonyl)phenylaminoacetyl]-8-methoxy-2H-chromen-2-one (15)

Yield: 66%; mp: 205−207 °C; ^{1}H NMR (200 MHz, DMSO-d$_6$), δ: 3.95 (s, 3H); 4.64 (d, 2H, J = 5.6 Hz); 6.27 (t, 1H, J = 5.6 Hz, exch. with D$_2$O); 6.84−6.88 (m, 1H); 7.16−7.19 (m, 3H); 7.32−7.56 (m, 3H); 8.74 (s, 1H); 12.69 (bs, 1H, exch. with D$_2$O). Anal. Calcd. for $C_{19}H_{15}NO_6$: C, 64.59; H, 4.28; N, 3.96; found: C, 64.71; H, 4.52; N, 4.06.

5.4. 3-(2-(3-(Hydroxycarbonyl)phenylamino)acetyl)-6-methoxy-2H-chromen-2-one (16)

Yield: 63%; mp: 205–207 °C; ^{1}H NMR (200 MHz, DMSO-d_6), δ: 3.82 (s, 3H); 4.65 (d, 2H, J = 5.2 Hz); 6.29 (t, 1H, J = 5.4 Hz, exch. with D_2O) 6.85–6.88 (m, 1H); 7.16–7.23 (m, 3H); 7.35–7.59 (m, 3H); 8.73 (s, 1H); 12.73 (bs, 1H, exch. with D_2O). Anal. Calcd. for $C_{19}H_{15}NO_6$: C, 64.59; H, 4.28; N, 3.96; found: C, 64.41; H, 4.36; N, 3.84.

5.5. 8-(Hydroxy-3-(2-(3-hydroxycarbonyl)phenylamino)acetyl)-2H-chromen-2-one (17)

Yield: 65%; mp: 217–219 °C; ^{1}H NMR (200 MHz, DMSO-d_6), δ: 4.60 (d, 2H, J = 4.6 Hz); 6.22 (t, 1H, J = 4.4 Hz, exch. with D_2O) 6.80–6.83 (m, 5H); 7.12–7.20 (m, 1H); 7.34–7.39 (m, 1H); 8.66 (s, 1H); 10.42 (s, 1H, exch. with D_2O); 12.64 (bs, 1H, exch. with D_2O). Anal. Calcd. for $C_{18}H_{13}NO_6$: C, 63.72; H, 3.86; N, 4.13; found: C, 63.91; H, 3.72; N, 4.16.

5.5. 6-(Chloro-3-(2-(3-hydroxycarbonyl)phenylamino)acetyl)-2H-chromen-2-one (18)

Yield: 80%; mp: 210–212 °C; ^{1}H NMR (200 MHz, DMSO-d_6): δ: 4.66 (d, 2H, J = 4.6 Hz); 6.29 (t, 1H, J = 4.6 Hz, exch. with D_2O) 6.87–6.88 (m, 1H); 7.16–7.20 (m, 3H); 7.54–7.61 (m, 1H); 7.76–7.87 (m, 1H); 8.14 (s, 1H); 8.73 (s, 1H); 12.70 (bs, 1H, exch. with D_2O). Anal. Calcd. for $C_{18}H_{12}ClNO_5$: C, 60.43; H, 3.38; N, 3.92; found: C, 60.61; H, 3.47; N, 4.05.

5.6. 6-(Chloro-3-(2-(3-hydroxycarbonyl)phenylamino)acetyl)-8-methoxy-2H-chromen-2-one (19)

Yield: 72%; mp: 213–215 °C; ^{1}H NMR (200 MHz, DMSO-d_6), δ: 3.98 (s, 3H); 4.64 (d, 2H, J = 4.2 Hz); 6.17 (t, 1H, J = 4.4 Hz, exch. with D_2O); 6.83–6.87 (m, 1H); 7.16–7.18 (m, 3H); 7.51 (s, 1H); 7.66 (s, 1H); 8.68 (s, 1H); 12.60 (bs, 1H, exch. with D_2O). Anal. Calcd. for $C_{19}H_{14}ClNO_6$: C, 58.85; H, 3.64; N, 3.61; found: C, 58.69; H, 3.53; N, 3.70.

5.7. 6-(Allyl-3-(2-(3-hydroxycarbonyl)phenylamino)acetyl)-8-methoxy-2H-chromen-2-one (20)

Yield: 69%; mp: 193–195 °C; ^{1}H NMR (200 MHz, DMSO-d_6), δ: 3.42 (d, 2H, J = 6.2 Hz); 3.95 (s, 3H); 4.61 (d, 2H, J = 4.0 Hz); 5.10–5.19 (m, 2H); 6.01–6.09 (m, 2H, 1H exch. with D_2O); 6.82–6.85 (m, 1H); 7.16–7.27 (m, 6H); 8.63 (s, 1H); 12.72 (bs, 1H, exch. with D_2O). Anal. Calcd. for $C_{22}H_{19}NO_6$: C, 67.17; H, 4.87; N, 3.56; found: C, 67.31; H, 4.73; N, 3.61.

6. General procedure for the synthesis of 3″,6,8-substituted 3-(2,3-dihydro-3-phenyl-2-thioxo-1H-imidazol-5-yl)-2H-chromen-2-one derivatives 1a-h

A mixture of compounds 13–20 (0.001 mol) and an excess of ammonium thiocyanate (1.14 g, 0.015 mol) in acetic acid (2 mL) was stirred for 1.5 h at 60–65 °C (TLC analysis). After cooling, the insoluble product was filtered off, washed with water, cold MeCN and cold diethyl ether to afford derivatives 1a-h in the desired purity degree (≥95%)

6.1. 3-(2,3-Dihydro-3-phenyl-2-thioxo-1H-imidazol-5-yl)-2H-chromen-2-one (1a)

Yield: 73%; mp: 255–257 °C (ref. [22]), mp: 154 °C. Anal. Calcd. for $C_{18}H_{12}N_2O_2S$: C, 67.48; H, 3.78; N, 8.74; found: C, 67.65; H, 3.59; N, 8.77.

6.2. 3-[2,3-(dihydro-3-(3-ethoxycarbonylphenyl)-2-thioxo-1H-imidazol-5-yl)]-2H-chromen-2-one] (1b)

Yield: 90%; mp: 260–262 °C; ^{1}H NMR (200 MHz, DMSO-d_6), δ: 1.34 (t, 3H, J = 7.0 Hz); 4.36 (q, 2H, J = 7.1 Hz); 7.40–7.50 (m, 2H); 7.63–7.74 (m, 3H); 7.91–8.05 (m, 3H); 8.25 (s, 1H); 8.59 (s, 1H); 13.18 (s, 1H, exch. with D_2O). Anal. Calcd. for $C_{21}H_{16}N_2O_4S$: C, 64.27; H, 4.11; N, 7.14; found: C, 64.45; H, 4.03; N, 7.27.

6.3. 3-[2,3-(dihydro-3-(3-hydroxycarbonylphenyl)-2-thioxo-1H-imidazol-5-yl)]-8-methoxy-2H-chromen-2-one (1c)

Yield: 62%; mp: >300 °C; ^{1}H NMR (200 MHz, DMSO-d_6), δ: 3.94 (s, 3H); 7.19–7.24 (m, 1H); 7.34–7.37 (m, 2H); 7.64–7.72 (m, 1H); 7.91–8.03 (m, 3H); 8.23 (s, 1H); 8.57 (s, 1H); 13.16 (bs, 2H, exch. with D_2O). Anal. Calcd. for $C_{20}H_{14}N_2O_5S$: C, 60.91; H, 3.58; N, 7.10; found: C, 61.05; H, 3.71; N, 7.06.

6.4. 3-[2,3-(dihydro-3-(3-hydroxycarbonylphenyl)-2-thioxo-1H-imidazol-5-yl)]-6-methoxy-2H-chromen-2-one (1d)

Yield: 87%; mp: >300 °C; ^{1}H NMR (200 MHz, DMSO-d_6), δ: 3.85 (s, 3H); 7.06–7.08 (m, 1H); 7.21–7.27 (m, 1H); 7.41–7.45 (m, 1H); 7.63–7.71 (m, 1H); 7.89–8.03 (m, 3H); 8.22 (s, 1H); 8.52 (s, 1H); 13.17 (bs, 1H, exch. with D_2O); 13.28 (bs, 1H, exch. with D_2O). Anal. Calcd. for $C_{20}H_{14}N_2O_5S$: C, 60.91; H, 3.58; N, 7.10; found: C, 60.85; H, 3.51; N, 7.22.

6.5. 3-[2,3-(dihydro-3-(3-hydroxycarbonylphenyl)-2-thioxo-1H-imidazol-5-yl)]-8-hydroxy-2H-chromen-2-one (1e)

Yield: 67%; mp: >300 °C; ^{1}H NMR (200 MHz, DMSO-d_6), δ: 7.06–7.28 (m, 3H, Ar-H); 7.63–7.71 (m, 1H); 7.89–8.03 (m, 3H); 8.23 (s, 1H); 8.53 (s, 1H); 10.37 (bs, 1H, exch. with D_2O); 13.13 (bs, 2H, exch. with D_2O). Anal. Calcd. for $C_{19}H_{12}N_2O_5S$: C, 59.99; H, 3.18; N, 7.36; found: C, 60.13; H, 3.23; N, 7.14.

6.6. 6-Chloro-3-[2,3-(dihydro-3-(3-hydroxycarbonylphenyl)-2-thioxo-1H-imidazol-5-yl)]-2H-chromen-2-one (1f)

Yield: 78%; mp: >300 °C; ^{1}H NMR (200 MHz, DMSO-d_6), δ: 7.50–7.54 (m, 1H); 7.64–7.71 (m, 3H); 7.92–8.04 (m, 3H); 8.22 (s, 1H); 8.48 (s, 1H); 13.23 (bs, 2H, exch. with D_2O). Anal. Calcd. for $C_{19}H_{11}ClN_2O_4S$: C, 57.22; H, 2.78; N, 7.02; found: C, 57.43; H, 2.77; N, 7.13.

6.7. 6-Chloro-3-[2,3-(dihydro-3-(3-hydroxycarbonylphenyl)-2-thioxo-1H-imidazol-5-yl)]-8-methoxy-2H-chromen-2-one (1g)

Yield: 71%; mp: >300 °C; ^{1}H NMR (200 MHz, DMSO-d_6): δ: 3.96 (s, 3H); 7.26 (s, 1H); 7.40 (s, 1H); 7.67–7.71 (m, 1H); 7.93–8.03 (m, 3H); 8.22 (s, 1H); 8.45 (s, 1H); 13.23 (bs, 2H, exch. with D_2O). Anal. Calcd. for $C_{20}H_{13}ClN_2O_5S$: C, 56.01; H, 3.06; N, 6.53; found: C, 56.23; H, 3.11; N, 6.42.

6.8. 6-Allyl-3-[2,3-(dihydro-3-(3-hydroxycarbonylphenyl)-2-thioxo-1H-imidazol-5-yl)]-8-methoxy-2H-chromen-2-one (1h)

Yield: 77%; mp: >300 °C; ^{1}H NMR (200 MHz, DMSO-d$_6$), δ: 3.49 (d, 2H, J = 6.0 Hz); 3.93 (s, 3H); 5.02–5.22 (m, 2H); 5.98–6.10 (m, 1H); 7.01 (s, 1H); 7.19 (s, 1H); 7.64–7.71 (m, 1H); 7.91–8.04 (m, 3H); 8.23 (s, 1H); 8.52 (s, 1H); 13.16 (bs, 2H, exch. with D$_2$O). Anal. Calcd. for C$_{23}$H$_{18}$N$_2$O$_5$S: C, 63.58; H, 4.18; N, 6.45; found: C, 63.39; H, 4.27; N, 6.71.

7. Biology. Materials and methods

Recombinant human MMP-14 catalytic domain was a kind gift of Prof. Gillian Murphy (Department of Oncology, University of Cambridge, UK). Pro-MMP-1, pro-MMP-2, pro-MMP-3, and pro-MMP-13 were purchased from Calbiochem. APMA was from Sigma-Aldrich. All compounds were subjected to combustion analysis prior to be tested for their inhibitory activity, to verify their consistence with a purity of at least 95%. ARP100 was synthesized at Department of Pharmaceutical Sciences (Pisa, Italy) according to the previously described procedure [23]. All other chemicals were of reagent grade.

7.1. Enzyme activation

Proenzymes were activated immediately prior to use with p-aminophenylmercuric acetate (APMA 2 mM for 1 h at 37 °C for MMP-2, APMA 2 mM for 2 h at 37 °C for MMP-1, 1 mM for 30 min at 37 °C for MMP-13). Pro-MMP-3 was activated with trypsin 5 μg/mL for 30 min at 37 °C followed by soybean trypsin inhibitor 62 μg/mL.

7.2. Enzyme inhibition assays

For assay measurements, the purchased compound stock solutions (10 mM in DMSO) were further diluted for each MMP in the fluorimetric assay buffer (FAB: Tris 50 mM, pH = 7.5, NaCl 150 mM, CaCl$_2$ 10 mM, Brij 35 0.05% and DMSO 1%). Activated enzyme (final concentration 0.56 nM for MMP-2, 0.3 nM for MMP-13, 5 nM for MMP-3, 1 nM for MMP-14cd, and 2.0 nM for MMP-1) and inhibitor solutions were incubated in the assay buffer for 4 h at 25 °C. After the addition of 200 μM solution of the fluorogenic substrate Mca-Arg-Pro-Lys-Pro-Val-Glu-Nva-Trp-Arg-Lys(Dnp)−NH$_2$ (Sigma) for MMP-3 and Mca-Lys-Pro-Leu-Gly-Leu-Dap(Dnp)-Ala-Arg−NH$_2$ (Bachem) for all the other enzymes in DMSO (final concentration 2 μM), the hydrolysis was monitored every 15 s for 15 min recording the increase in fluorescence ($λ_{ex}$ = 325 nm, $λ_{em}$ = 395 nm) using a Molecular Devices SpectraMax Gemini XS plate reader. The assays were performed in triplicate in a total volume of 200 μL per well in 96-well microtitre plates (Corning, black, NBS). The MMP inhibition activity was expressed in relative fluorescent units (RFU). Percent of inhibition was calculated from control reactions without the inhibitor. The inhibitory effect of the tested compounds was routinely estimated at a concentration of 100 μM towards MMP-13. Those derivatives found to be active were tested at additional concentrations and IC$_{50}$ was determined using at least five concentrations of the inhibitor causing an inhibition between 10% and 90%, using the formula: $V_i/V_o = 1/(1 + [I]/IC_{50})$, where V_i is the initial velocity of substrate cleavage in the presence of the inhibitor at concentration [I] and V_o is the initial velocity in the absence of the inhibitor. Results were analyzed using SoftMax Pro software [24] and Origin 6.0 software.
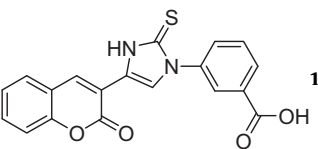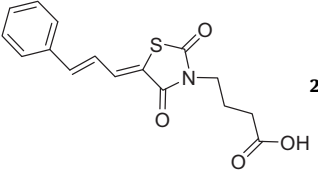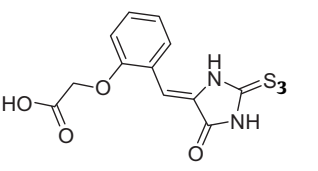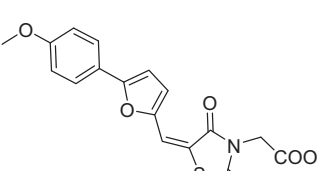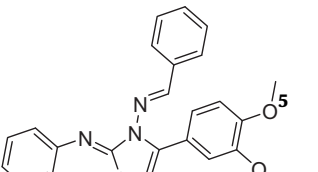
8. Results and discussion

8.1. Virtual screening

To date, several X-ray structures of MMP-13 have been released in the Protein Data Bank. Besides that co-crystallized with TIMP-2 (PDB code: 2E2D), all the others were co-crystallized with organic inhibitors such as the diphenylether sulfone RS-130830 (PDB code 830C). A superposition of all X-ray structures on the alpha carbon atoms, using 830C as reference structure, shows that the protein folding and the catalytic loops shape are highly superimposable, and that in the catalytic site the large majority of the residues are all preserved in the side chain conformations. Thus, only the enzyme structure 830C, which has the higher resolution (1.60 Å), was selected for our VS experiment. As docking program for the VS, we used the Autodock program (AD4) [25], which has been extensively and successfully employed in multiple VS campaigns undertaken by our research group [26]. AD4 was applied to virtually screen the Life Chemicals database, a collection of six thousands non-redundant drug-like compounds selected to provide the broadest pharmacophore coverage. Prior to docking experiments, the entire Life Chemicals database was processed with the ZINC protocol leading to a total of 7769 molecules (see Experimental section for details). The results of the VS on the Life Chemical database, were then sorted on the basis of the predicted binding free energies ($ΔG_{AD4}$) which in our case ranged from −3.93 to −15.61 kcal/mol. A scoring filter was set arbitrarily to −10.5 kcal/mol so as to retain 23% of the docked solutions. The top 1800 compounds in their predicted binding poses were selected for visual inspection. In order to obtain compounds endowed with an inhibitory potency against MMP-13, we discarded all the molecules for which AD4 did not predict coordination of the catalytic zinc. Then, in the attempt to find leads with a certain selectivity of action, for each inspected compound, the occupancy of the S1′ pocket has been evaluated, although it was not expected to be total due to the small size of the docked compounds. As last criterion of choice, we evaluated the attitude of each molecule to be chemically optimized. At the end of this process, a total of 24 compounds of the Life Chemical Data Set were selected for further analysis. Two products were not available from the vendor, and two were not soluble at the test concentration, so a total of twenty compounds were used for biochemical assays. Initially, all compounds were screened at a concentration of 100 μM by fluorometric assay on recombinat enzyme. ARP100 [23], a hydroxamate-based MMP inhibitor previously developed by our research group, was used in the same assay conditions as reference compound. To exclude any possible nonspecific/promiscuous inhibition of MMP-13 due to aggregate formation, we performed all the assays pertaining the active compounds in the presence of 0.05% Brij-35, a nonionic detergent similar to Triton X-100, as suggested by Shoichet et al. [27]. Five ligands, out of the twenty tested, provided considerable inhibition of MMP-13 activity and were characterized in detail (see experimental methods). All other compounds that did not cause detectable inhibition at 100 μM concentrations were not further investigated (see SI for chemical structures). Table 1 lists structures, Life Chemicals codes, AD4 binding free energies and the MMP-13 IC$_{50}$ of the novel inhibitors which ranges from 9 to 140 μM. The IC$_{50}$ values were deduced from the non linear regression analysis of the log dose response curves (see Supporting Information).

As shown in Table 1, all inhibitors scaffolds are structurally diverse from each other and from most of the known MMPIs. With the exception of 5 (and maybe 4, see paragraph "Active Compounds Binding Modes and Hints for Lead Optimization"), all active compounds possess a carboxylate function as ZBG. Compound 5 which holds a dimethoxybenzene as ZBG retains a certain activity

Table 1
Structures, labels, AD4 binding free energies and IC$_{50}$ of MMP-13 inhibitors identified with VS experiments.

Chemical structure	Life chemicals code	ΔG$_{AD4}$ (Kcal/mol)	IC$_{50}$ (μM)[a]
1	F0920-6501	−13.33	14
2	F1074-0280	−13.12	22
3	F1204-0078	−10.96	67
4	F1542-0089	−12.11	120
5	F0807-0342	−10.5	140

[a] IC$_{50}$ values represent the concentration required to produce 50% enzyme inhibition.

although his IC$_{50}$ (140 μM) is higher than all of the carboxylate-containing inhibitors. Recently, Novartis researchers reported that a series of carboxylic acids such as the MMP-13 inhibitor **24f** [28] were orally available and equipotent to the most potent hydroxamic acid based inhibitors in *in vivo* models of cartilage protection. Thus, some key physicochemical properties, such as pKa, ClogP, ClogD, and TPSA, were *in silico* calculated for our five leads and compared to those of **24f** (Table 2) [29]. As shown in Table 2, with the exception of **5**, which seems to be the least drug-like compound, all other inhibitors possess an average value of ClogP ranging from 0.89 to 3.32 and a ClogD and a TPSA very similar to that of **24f**. Thus, with the exception of **5**, all the others seem to be suitable leads, for which the S1′ substituent could be easily extended and/or modified.

Table 2
In silico calculated physicochemical properties of compounds **1–5** and **24f**.

Compd	pKa [a]	ClogP [b]	ClogD [c]	TPSA (Å) [d]
1	3.91	3.32	0.11	119.96
2	3.89	2.6	−0.61	99.98
3	3.68	0.89	−2.56	119.75
4	3.62	2.91	−0.42	137.37
5	–	5.55	5.55	71.71
24f[e]	2.55	3.39	−0.13	158.86

[a] pKa predictions refers to the ZBG.
[b] Calculated n-octanol/water partition coefficient.
[c] Calculated distribution coefficient at pH = 7.4.
[d] Topological polar surface area.
[e] Orally active carboxylic acid-derived MMP-13 inhibitor used for comparison purpose [19].

Table 3
In Vitro[a] activity (IC$_{50}$ μM values) of the novel MMP-13 inhibitors towards diverse MMPs.

Compd	Life chemicals code	MMP-1	MMP-2	MMP-3	MMP-13	MMP-14
1	F0920-6501	400 ± 150	67 ± 3.0	110 ± 15	14 ± 0.5	51 ± 7.0
2	F1074-0280	93 ± 8.0	2.7 ± 0.2	110 ± 26	22 ± 0.6	21 ± 2.0
3	F1204-0078	114 ± 23	61 ± 7.0	77 ± 21	67 ± 10	55 ± 4.0
4	F1542-0089	860 ± 110	350 ± 38	850 ± 200	120 ± 8	310 ± 18
5	F0807-0342	360 ± 46	120 ± 14	230 ± 24	140 ± 10	150 ± 18

[a] Assays were run in triplicate. The final values given here are the mean ±SD of three independent experiments.
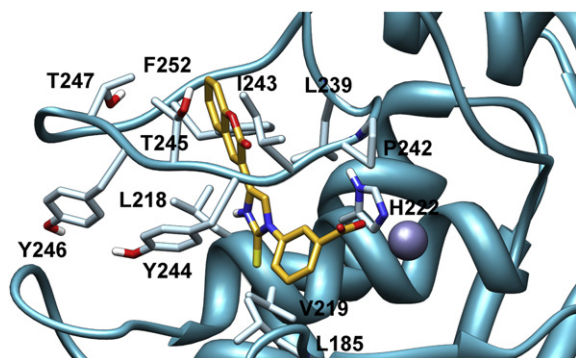
Fig. 1. Docked conformations of **1** in the MMP-13 catalytic site. Hydrogen atoms are omitted for the sake of clarity. Ligands carbon atoms are displayed in golden, and key binding site residues as cyan sticks.

8.2. Biological evaluation

The inhibitory activity of the five novel leads was evaluated (Table 3) against a panel of MMP isozymes (MMP-1, -2, -3, -13, -14), some of which are implicated in cartilage degradation. Over the five inhibitors, two (**1** and **4**) are definitely more active on MMP-13 showing appreciably weaker activity on all the other tested enzymes (Table 3). In this respect, both compounds represent appealing leads amenable of structural modification to develop selective MMP-13 inhibitors. Inhibitors **3**, and **5** are equally active on MMP-13 and MMP-14. The two compounds show inhibitory activity also towards MMP-2. In this respect, it is not clear whether this inhibitory profile is beneficial in terms of protecting cartilage degradation. Actually, the role of MMP-2 activity itself in the pathogenesis of OA is unclear. Interestingly, mRNA levels of MMP-2 are increased in OA patients compared to normal controls, suggesting that MMP-2 may play a role in this disease [30]. On the other hand, MMP-2-null mice exhibit a more severe arthritic phenotype than wild type mice in antigen-induced arthritis, suggesting that the total loss of MMP-2 activity is unfavourable [31]. Differently, compound **2** shows a certain preference for MMP-2 ($IC_{50} = 2.7$ μM) and could be developed as novel antitumor agent.

8.3. Active compounds binding modes and general hints for leads optimization

Besides the carboxylate function, which, with the exception of **5**, is a conserved feature of all active inhibitors, the five compounds deeply differ in their chemical structures. Indeed, in **1**, the carboxylate moiety is directly attached to a benzene ring, in **2** this portion is linked to a thiazolidinedione nucleus by a propyl-linker, while in **3** and **4** a oxymethylene and a methylene bridge link the carboxylate group to a benzene and thioxothiazolidinone ring, respectively. Regardless the structural dissimilarities among the aforementioned ligands, all of them are characterized by a small number of rotatable bonds (ranging from 0 to 4). Indeed, the rigidity of **1** allows the proper orientation of the ZBG to chelate the catalytic zinc ion and the P1′ group into the S1′ pocket (see Fig. 1). The imidazolethione ring is in a suitable position to establish a π—π interaction with H222 side chain. The micromolar IC_{50} for this compound might be due to the non-optimized interaction between the P1′ group and the S1′ pocket and to a too high rigidity. The selectivity of **1** towards the MMP-13 is surely ascribable to the bulky chromenone nucleus located into the unusually large S1′ specificity pocket. In fact, although MMP-13 and -14 possess a S1′ specificity loop of the same length, the latter has a narrower shaped S1′ pocket, due to the substitution of T245 and T247 in MMP-13
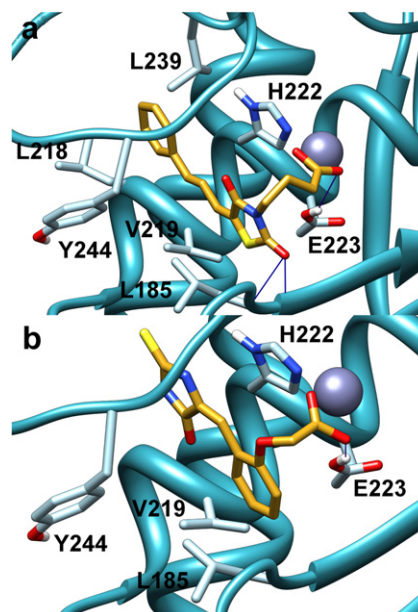

Fig. 2. Docked conformations of **2** (a) and **3** (b) In the MMP-13 catalytic site.

with Q262 and M264 in MMP-14. This hypotheses is confirmed by inhibitor **2** (Fig. 2a), which shows the same activity on MMP-13 and MMP-14 possessing a thin olefinic chain ending with a phenyl ring which is unable to fill the roomy S1′ pocket. Differently from inhibitor **2**, compound **3** has a small and polar P1′ group, and this is the reason for the lower activity and selectivity for MMP-13 with respect to **1** and **2**. However in **3** (Fig. 2b), the thioxoimidazolidinone ring could be substituted with groups featuring shapes and electrostatic propertied able to favourably interact with the peculiar S1′ tunnel of MMP-13. Especially for this compound, the extension of the P1′ group is certainly a priority step.

As regards compound **4** (Fig. 3a), molecular docking unambiguously indicate that the ZBG would be the carboxylate group and not the rhodanine ring via the thiazolidine sulphur atom, as
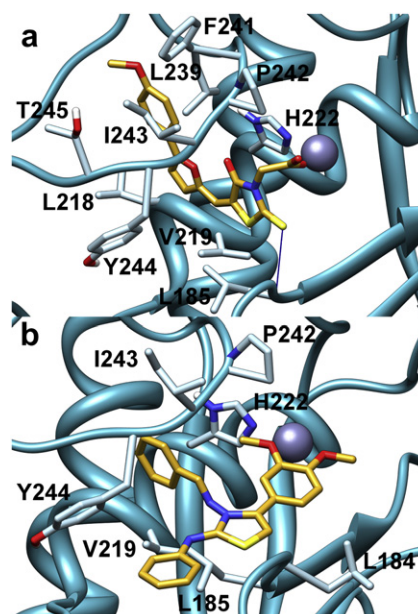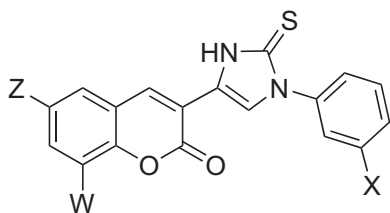

Fig. 3. Docked conformations of **4** (a) and **5** (b) In the MMP-13 catalytic site.

Table 4
Chemical structure and inhibitor activity of compound **1** and the prepared compounds.

Chemical structure	W	Z	X	IC$_{50}$ (μM)
1	H	H	COOH	14 ± 1.4
1a	H	H	H	177 ± 14
1b	H	H	COOCH$_2$CH$_3$	>300
1c	OCH$_3$	H	COOH	5.2 ± 1.1
1d	H	OCH$_3$	COOH	3.2 ± 0.2
1e	OH	H	COOH	5.5 ± 1.1
1f	H	Cl	COOH	2.6 ± 0.6
1g	OCH$_3$	Cl	COOH	4.9 ± 0.6
1h	OCH$_3$	CH$_2$CH=CH$_2$	COOH	4.9 ± 0.8

previously found for anthrax lethal factor inhibitors [32], which have in common with compound **4** both the rhodanine ring and the carboxylate group. However, a search in the Cambridge Structural Databases shows that, at least in absence of any receptor structure, the carboxylate moiety prevails onto the rhodanine ring in the coordination of metal ions. Thus, prior of any rational optimization, further studies have to be conducted in order to assess the real binding mode of **4** in the MMP-13 active site.

Inhibitor **5** (Fig. 3b), is the weakest inhibitor (IC$_{50}$ on MMP-13 = 140 μM) on the entire panel of MMPs tested, although it is the only one whose P1′ group is able to make some contacts with the entrance residues of the S1′ pocket like P242, V219, as well as a parallel π-stacking with the H222. The thiazolidine ring makes some lipophilic contacts with the S1′ pocket floor residues (L184 and L185), while the N-benzylidene group projects itself towards the beta carbons of the Y244 and the I243.
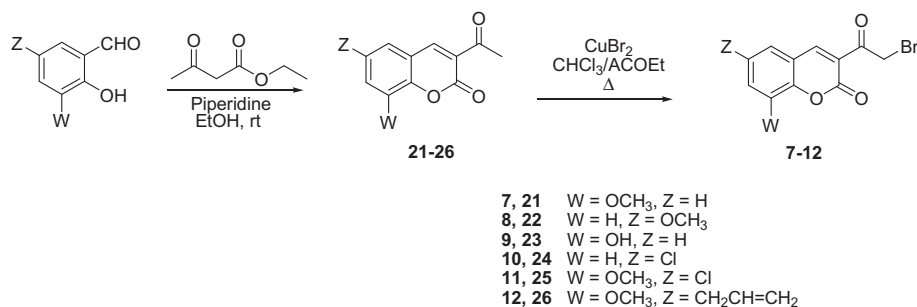
In this case, the low activity is ascribable to the presence of a putative weak zinc ion chelator (dimethoxybenzene) and to the fact that it has been tested as a mixture of diastereoisomers. Thus, separation and testing of each single diastereoisomer, together with the substitution of the weak chelator moiety with a stronger one, could be the first step of the lead optimization process of this inhibitor. Subsequent steps could include proper substitutions of both phenyl rings to enhance the interaction with the S1′ and S3′ pockets.
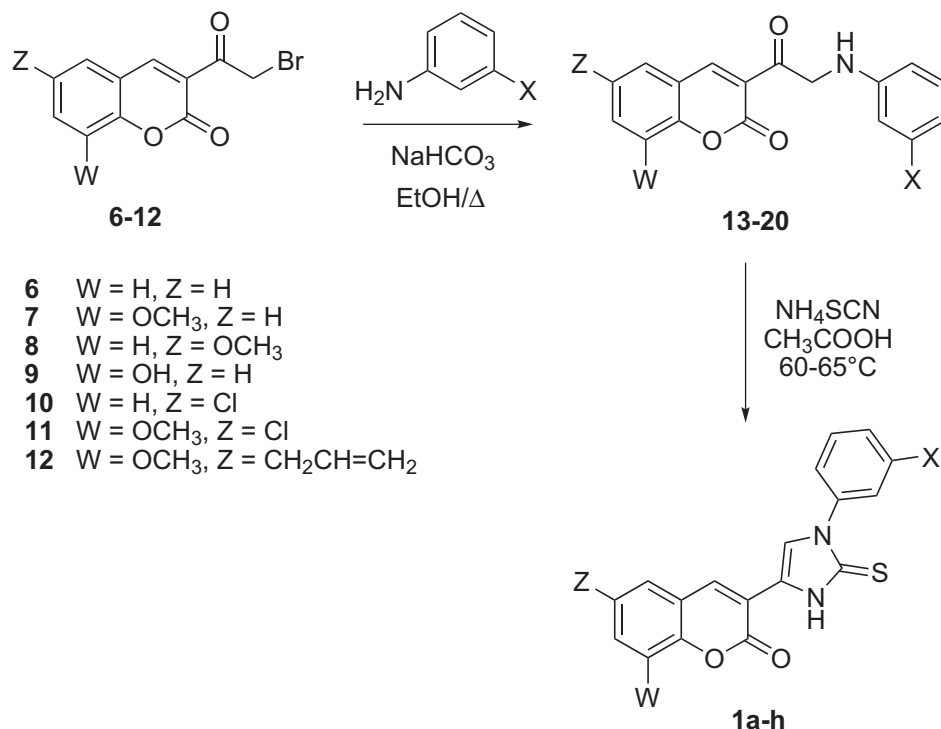
6	W = H, Z = H	
7	W = OCH$_3$, Z = H	
8	W = H, Z = OCH$_3$	
9	W = OH, Z = H	
10	W = H, Z = Cl	
11	W = OCH$_3$, Z = Cl	
12	W = OCH$_3$, Z = CH$_2$CH=CH$_2$	

13, **1a**	W = H, Z = H, X = H	
14, **1b**	W = H, Z = H, X = COOCH$_2$CH$_3$	
15, **1c**	W = OCH$_3$, Z = H, X = COOH	
16, **1d**	W = H, Z = OCH$_3$, X = COOH	
17, **1e**	W = OH, Z = H, X = COOH	
18, **1f**	W = H, Z = Cl, X = COOH	
19, **1g**	W = OCH$_3$, Z = Cl, X = COOH	
20, **1h**	W = OCH$_3$, Z = CH$_2$CH=CH$_2$, X = COOH	

Scheme 1.

Scheme 2.

7, 21   W = OCH$_3$, Z = H
8, 22   W = H, Z = OCH$_3$
9, 23   W = OH, Z = H
10, 24 W = H, Z = Cl
11, 25 W = OCH$_3$, Z = Cl
12, 26 W = OCH$_3$, Z = CH$_2$CH=CH$_2$

Thus, generally speaking, none of these compounds has such an extended P1′ group to occupy the whole S1′ tunnel of the MMP-13, neither the P1′ are well-optimized to interact with the pocket. This is certainly the reason for the inhibitory activities in the range of μM. However, a rationally designed lead optimization project will surely increase the experimental IC$_{50}$. In fact, even if less potent than hydroxamate-based inhibitors, carboxylates could be a valid alternative to this moiety. This weaker zinc-binder could allow to have selective inhibition if present in properly optimized structures. For **1** and **4**, which show a pretty good selectivity profile, lead optimizations are already an ongoing projects. Herein we reported the first round of structure-based optimization on lead **1**.

8.4. Receptor-based lead optimization of **1**

As first step in our lead optimization process we verified the reliability of the proposed binding mode, synthetizing and testing the decarboxylated analogue (**1a**) and the ethyl ester derivative (**1b**) of compound **1**. The IC$_{50}$ obtained of **1a** and **1b** (Table 4) fully substantiate that the carboxylate group binds the catalytic zinc ion as predicted by the docking program. As next step, the first round of lead optimization was rationally carried out by taking into account the theoretical binding pose of **1** in the MMP-13 binding site. As aforesaid, the rigidity of **1** allows the proper orientation of the ZBG to chelate the catalytic zinc ion and the P1′ group into the S1′ pocket, while the imidazolethione ring establishes a π−π interaction with H222 side chain. Thus, the micromolar IC$_{50}$ for this compound might be ascribed to the non-optimized interaction between the P1′ group and the S1′ pocket. In the first step of lead optimization we decided to explore positions 6- and 8- of the chromenone ring, while positions 4- and 5- will be object of a next round of optimization. However, it has to be said that close to the inhibitor core there is the L218 (distance between hydrogen in position 4- and L218 β carbon is 3.60 Å, distance between hydrogen in position 5- and δ1 carbon of L218 is 3.20 Å) which would not tolerate bulky substituents. On the basis of the proposed binding mode, substitutions on position 7 should not help in increasing the number of interactions with the enzyme as this position is solvent exposed. Thus, in the attempt to allow **1** to establish further contacts with the upper part of the S1′-specificity loop, eg. an H-bond with the A238 carbonyl oxygen or an hydrophobic interaction with the P255 side chain the 8-OH (**1e**) and the 8-OCH$_3$ (**1c**) derivatives were respectively prepared (Table 4). These small modifications to **1** were successful in lowering the IC$_{50}$ (Table 4). Furthermore, with the aim of enhancing the lipophilic interactions with F252 and T247, at the bottom of the S1′ pocket, the 6-OCH$_3$ (**1d**) and 6-Cl (**1f**) derivatives were synthesized. In this case the improvement in the inhibition toward the MMP-13 was even higher with an IC$_{50}$ of 3.2 μM and 2.6 μM, correspondingly. However, a close inspection of the binding mode predicted for **1**,

which has been fully confirmed by this first round of optimization, suggests that for further activity optimization, more flexibility has to be conferred to **1**. Thus, design and synthesis of novel, more flexible, derivatives will be the next step of our research program and it is expected to led to the desired activity.

8.5. Chemistry

The general procedure for the synthesis of the target inhibitors **1a**−**h** involved the reaction of the 3-bromoacetylcoumarin derivatives **6**−**12** with the appropriate arylamine (aniline, 3-aminobenzoic acid, ethyl 3-aminobenzoate) in ethanol at room temperature for 5 h (TLC analysis), in the presence of NaHCO$_3$, to yield products **13**−**20** (Scheme 1), which crystallized pure by cooling the reaction mixture. Derivatives **1a**−**h** were then obtained by treatment of compounds **13**−**20** with a large excess of ammonium thiocyanate in acetic acid at 60−65 °C for 1.5 h (TLC analysis). After work-up of the reaction, washing with water, cold acetonitrile, and cold diethyl ether, derivatives **1a**−**h** were directly obtained with the desired purity degree (≥95%). The 3-bromoacetylcoumarin **6** is commercially available. The substituted coumarin derivatives **7**−**12** were easily prepared as outlined in Scheme 2. Following a reported procedure with slight modifications, the 3-acetylcoumarins **21**−**26** were obtained by a Knoevenagel condensation of the appropriate salicylaldehyde (2-hydroxy-3-methoxybenzaldehyde, 2-hydroxy-5-methoxybenzaldehyde, 2,3-dihydroxybenzaldehyde, 5-chloro-2-hydroxybenzaldehyde, 5-chloro-2-hydroxy-3-methoxybenz aldehyde, 5-allyl-2-hydroxy-3-methoxybenzaldehyde) and ethyl acetoacetate, using piperidine as a catalyst in absolute ethanol at room temperature for 5 h (TLC analysis) (Scheme 2), Crystallization from ethanol gave the pure products **21**−**26**. These latter compounds were then transformed into the corresponding 2-bromoacetyl derivatives **7**−**12** by treatment with copper (II) bromide and reflux in chloroform-ethyl acetate. The reaction was complete as judged by a colour change of the solution from green to amber, disappearance of all black solid, and cessation of hydrogen bromide evolution. Products **7**−**12** were finally purified by crystallization from ethanol.

9. Conclusions

This paper reports the identification of structurally non-classic MMP-13 inhibitors by means of an *in silico* screening of 7769 compounds to the active site of the enzyme. Experimental evaluation of 20 candidates, which were selected by visual inspection of the poses predicted for the best scoring compounds, led to the identification of five novel zinc-chelating non-hydroxamate inhibitors, structurally distinct from those already reported. All five may provide scaffolds upon which to develop compounds with more desirable properties, such as selectivity of action and oral availability. A first round of structure-based optimization on lead **1** was

accomplished and led to an increase in potency of more than 5 fold. The next round of optimization, where more flexible derivatives will be designed and synthesized is expected to lead to the desired activity. Finally the herein reported work demonstrated that the use of virtual screening can represent a successful method for the discovery of novel MMPIs with a chemical structure diverse from each other and from most of the known MMPIs.

Appendix. Supplementary material

Supplementary data related to this article can be found online at doi:10.1016/j.ejmech.2011.10.035.

References

[1] J.S. Mort, C.J. Billington, Articular cartilage and changes in arthritis: matrix degradation, Arthritis Res. 3 (2001) 337—341.
[2] (a) A. Jüngel, C. Ospelt, M. Lesch, M. Thiel, T. Sunyer, O. Schorr, B.A. Michel, R.E. Gay, C. Kolling, C. Flory, S. Gay, M. Neidhart, Effect of the oral application of a highly selective MMP-13 inhibitor in three different animal models of rheumatoid arthritis, Ann. Rheum. Dis. 69 (2010) 898—902;
(b) N.G. Li, Z.H. Shi, Y.P. Tang, Z.J. Wang, S.L. Song, L.H. Qian, D.W. Qian, J.A. Duan, New hope for the treatment of osteoarthritis through selective inhibition of MMP-13, Curr. Med. Chem. 18 (2011) 977—1001.
[3] (a) M. Sabatini, C. Lesur, M. Thomas, A. Chomel, P. Anract, G. deNanteuil, P. Pastoureau, Effect of inhibition of matrix metalloproteinases on cartilage loss in vitro and in a guinea pig model of osteoarthritis, Arthritis Rheum. 52 (2005) 171—180.(b)V.M. Baragi, G. Becher, A.M. Bendele, R. Biesinger, H. Bluhm, J. Boer, H. Deng, R. Dodd, M. Essers, T. Feuerstein, B.M. Gallagher, C. Gege, M. Hochgürtel, M. Hofmann, A. Jaworski, L. Jin, A. Kiely, B. Korniski, H. Kroth, D. Nix, B. Nolte, D. Piecha, T.S. Powers, F. Richter, M. Schneider, C. Steeneck, I. Sucholeiki, A. Taveras, A. Timmermann, J. Van Veldhuizen, J. Weik, X. Wu, B. Xia, A new class of potent matrix metalloproteinase 13 inhibitors for potential treatment of osteoarthritis: evidence of histologic and clinical efficacy without musculoskeletal toxicity in rat models, Arthritis Rheum. 60 (2009) 2008—2018.
[4] R. Renkiewicz, L. Qiu, C. Lesch, X. Sun, R. Devalaraja, T. Cody, E. Kaldjian, H. Welgus, V. Baragi, Broad-spectrum matrix metalloproteinase inhibitor marimastat-induced musculoskeletal side effects in rats, Arthritis Rheum. 48 (2003) 1742—1749.
[5] H. Wu, J. Du, Q. Zheng, Expression of MMP-1 in cartilage and synovium of experimentally induced rabbit ACLT traumatic osteoarthritis: immunohisto-chemical study, Rheumatol. Int. 29 (2008) 31—36.
[6] J.J. Li, J. Nahra, A.R. Johnson, A. Bunker, P. O0Brien, W.S. Yue, D.F. Ortwine, C.F. Man, V. Baragi, K. Kilgore, R.D. Dyer, H.K. Han, Quinazolinones and pyrido-[3,4-d]pyrimidin-4-ones as orally active and specific matrix metalloproteinase-13 inhibitors for the treatment of osteoarthritis, J. Med. Chem. 51 (2008) 835—841.
[7] E. Nuti, F. Casalini, S.I. Avramova, S. Santamaria, G. Cercignani, L. Marinelli, V. La Pietra, E. Novellino, E. Orlandini, S. Nencetti, T. Tuccinardi, A. Martinelli, N.H. Lim, R. Visse, H. Nagase, A. Rossello, N—O—isopropyl sulfonamido-based hydroxamates: design, synthesis and biological evaluation of selective matrix metalloproteinase-13 inhibitors as potential therapeutic agents for osteoar-thritis, J. Med. Chem. 52 (2009) 4757—4773.
[8] M. Flipo, J. Charton, A. Hocine, S. Dassonneville, B. Deprez, R. Deprez-Poulain, Hydroxamates: relationships between structure and plasma stability, J. Med. Chem. 52 (2009) 6790—6802.
[9] E. Nuti, L. Panelli, F. Casalini, S.I. Avramova, E. Orlandini, S. Santamaria, S. Nencetti, T. Tuccinardi, A. Martinelli, G. Cercignani, N. D'Amelio, A. Maiocchi, F. Uggeri, A. Rossello, Design, synthesis, biological evaluation, and NMR studies of a new series of arylsulfones as selective and potent matrix metalloproteinase-12 inhibitors, J. Med. Chem. 52 (2009) 6347—6361.
[10] www.lifechemicals.com
[11] http://zinc.docking.org
[12] R. Huey, G.M. Morris, A.J. Olson, D.S. Goodsell, A semiempirical free energy force field with charge-based desolvation, J. Comput. Chem. 28 (2007) 1145—1152.
[13] E.F. Pettersen, T.D. Goddard, C.C. Huang, G.S. Couch, D.M. Greenblatt, E.C. Meng, T.E. Ferrin, UCSF, Chimera—a visualization system for exploratory research and analysis, J. Comput. Chem. 25 (2004) 1605—1612.
[14] (a) S. Stanchev, G. Momekov, F. Jensen, I. Manolov, Synthesis, computational study and cytotoxic activity of new 4-hydroxycoumarin derivatives, Eur. J. Med. Chem. 43 (2008) 694—706;

[15] (b) E.C. Horning, M.G. Horning, Coumarins from 2-hydroxy-3-methoxybenzaldehyde, J. Am. Chem. Soc. 69 (1947) 968—969.
[15] I.Y. Flores-Larios, L. Lopez-Garrido, F.J. Martinez-Martinez, J. Gonzalez, E.V. Garcia-Baez, A. Cruz, I.I. Padilla-Martinez, Thermal [4+2] cycloadditions of 3-acetyl-, 3-carbamoyl-, and 3-ethoxycarbonyl-coumarins with 2,3-dimethyl-1,3-butadiene under solventless conditions: a structural study, Molecules 15 (2010) 1513—1530.
[16] X. Liu, J. Fan, Y. Liu, Z. Shang, L-Proline as an efficient and reusable promoter for the synthesis of coumarins in ionic liquid, J. Zhejiang Univ. Sci. B 9 (2008) 990—995.
[17] X. Liu, J. Fan, Y. Liu, Z. Shang, L-proline as an efficient and reusable promoter for the synthesis of coumarins in ionic liquid, J. Zhejiang Univ. Sci. B 9 (2008) 990—995.
[18] V.R. Rao, T.V.P. Rao, Studies on coumarin derivatives. Part I. Synthesis of some substituted thiazolyl and benzoxazinylcoumarins, Indian J. Chem. Sect. B. Org. Chem. Including Med. Chem. 25 (1986) 413—415.
[19] C. Murata, T. Masuda, Y. Kamochi, K. Todoroki, H. Yoshida, H. Nohta, M. Yamaguchi, A. Takadate, Improvement of fluorescence characteristics of coumarins: syntheses and fluorescence properties of 6-methoxycoumarin and benzocoumarin derivatives as novel fluorophores emitting in the longer wavelength region and their application to analytical reagents, Chem. Pharm. Bull. 53 (2005) 750—758.
[20] G.K. Rao, K.N. Venugopala, P.N.S. Pai, Microwave-assisted synthesis of some 6-chloro-3-[2-(substitutedanilino)-1,3-thiazol-4-yl]-2H-1-benzopyran-2-ones as antibacterial agents, Indian J. Heterocyclic Chem. 17 (2008) 397—400.
[21] C.F. Koelsch, Bromination of 3-acetocoumarin, J. Am. Chem. Soc. 72 (1950) 2993—2995.
[22] S.S. Soman, T.H. Thaker, Synthesis of new 3-(1-aryl-2-thioxo-3,4-dihydro-2H-imidazol-4-yl)chromen-2-ones, Indian J. Heterocyclic Chem. 19 (2009) 55—58.
[23] A. Rossello, E. Nuti, E. Orlandini, P. Carelli, S. Rapposelli, M. Macchia, F. Minutolo, L. Carbonaro, A. Albini, R. Benelli, G. Cercignani, G. Murphy, A. Balsamo, New N-arylsulfonyl-N-alkoxyaminoacetohydroxamic acids as selective inhibitors of gelatinase A (MMP-2), Bioorg. Med. Chem. 12 (2004) 2441—2450.
[24] SoftMax Pro 4.7.1 by Molecular Devices.
[25] S.F. Sousa, P.A. Fernandes, M.J. Ramos, Protein—ligand docking: current status and future challenges, Proteins 65 (2006) 15—26.
[26] (a) S. Cosconati, L. Marinelli, R. Trotta, A. Virno, L. Mayol, E. Novellino, A.J. Olson, A. Randazzo, Tandem application of virtual screening and NMR experiments in the discovery of brand new DNA quadruplex groove binders, J. Am. Chem. Soc. 131 (2009) 16336—16337;
(b) S. Cosconati, J.A. Hong, E. Novellino, K.S. Carroll, D.S. Goodsell, A.J. Olson, Structure-based virtual screening and biological evaluation of Mycobacterium tuberculosis adenosine 5'-phosphosulfate reductase inhibitors, J. Med. Chem. 51 (2008) 6627—6630;
(c) S. Cosconati, L. Marinelli, C. La Motta, F. Sartini, F. Da Settimo, A.J. Olson, E. Novellino, Pursuing aldose reductase inhibitors through in situ cross-docking and similarity-based virtual screening, J. Med. Chem. 52 (2009) 5578—5581.
[27] (a) S.L. McGovern, E. Caselli, N. Grigorieff, B.K. Shoichet, A common mecha-nism underlying promiscuous Inhibitors from virtual and high-throughput screening, J. Med. Chem. 45 (2002) 1712—1722;
(b) S.L. McGovern, B.T. Helfand, B. Feng, B.K. Shoichet, A specific mechanism of non-specific inhibition, J. Med. Chem. 46 (2003) 4265—4272.
[28] L.G. Monovich, R.A. Tommasi, R.A. Fujimoto, V. Blancuzzi, K. Clark, W.D. Cornell, R. Doti, J. Doughty, J. Fang, D. Farley, J. Fitt, V. Ganu, R. Goldberg, R. Goldstein, S. Lavoie, R. Kulathila, W. Macchia, D.T. Parker, R. Melton, E. O'Byrne, G. Pastor, T. Pellas, E. Quadros, N. Reel, D.M. Roland, Y. Sakane, H. Singh, J. Skiles, J. Somers, K. Toscano, A. Wigg, S. Zhou, L. Zhu, W.C. Shieh, S. Xue, L.W. McQuire, Discovery of potent, selective, and orally active carboxylic acid based inhibitors of matrix metalloproteinase-13, J. Med. Chem. 52 (2009) 3523—3538.
[29] The pKa, CLogP, CLogD calculations were performed with the chemsilico server on the web site: http://chemsilico.com. The TPSA calculation was performed with marvin sketch and calculator plugins on the web-site: http://www.chemaxon.com/demosite/marvin/index.html.
[30] L. Kevorkian, D.A. Young, C. Darrah, S.T. Donell, L. Shepstone, S. Porter, S.M. Brockbank, D.R. Edwards, A.E. Parker, I.M. Clark, Expression profiling of metalloproteinases and their inhibitors in cartilage, Arthritis Rheum. 50 (2004) 131—141.
[31] T. Itoh, H. Matsuda, M. Tanioka, K. Kuwabara, S. Itohara, R. Suzuki, The role of matrix metealloproteinase-2 and matrix metalloproteinase-9 in antibody induced arthritis, J. Immunol. 169 (2002) 2643—2647.
[32] S.L. Johnson, D. Jung, M. Forino, Y. Chen, A. Satterthwait, D.V. Rozanov, A.Y. Strongin, M. Pellecchia, Anthrax lethal factor protease inhibitors: synthesis, SAR, and structure-based 3D QSAR studies, J. Med. Chem. 49 (2006) 27—30.